CHEBYSHEV FILTER APPLIED TO AN INVERSION TECHNIQUE FOR BREAST TUMOUR DETECTION

Marta A P Elizabeth[1], Kismet Anak Hong Ping[2], Nordiana Binti Rajaee[3], Toshifumi Moriyama[4]

[1]PG Student, Department of Electrical and Electronic Engineering, Faculty of Engineering, Universiti Malaysia Sarawak,Jalan Datuk Mohd Musa, 94300 Kota Samarahan, Sarawak,MALAYSIA
[2-3]Senior Lecturer, Department of Electrical and Electronic Engineering, Faculty of Engineering, Universiti Malaysia Sarawak, Jalan Datuk Mohd Musa, 94300 Kota Samarahan, Sarawak, MALAYSIA
[4]Associate Professor, Department of Electrical and Electronic Engineering, Faculty of Engineering, Nagasaki University,1-14 Bunkyo-machi, Nagasaki 852-8521, JAPAN

Abstract

Microwave imaging has been extensively studied in the past several years as a new technique for early stage breast cancer detection. The rationale of microwave imaging for breast tumour detection is significant contrast in the dielectric properties of normal tissue and malignant tumours. However, in practice noise present from the environments during screening/examination degrades the quality of the image. Inaccurate reconstructed image caused false/misleading interpretation of the image which leads to inappropriate diagnose or treatment to the patient. In the simulation works, noise is added to imitate the actual environment scenario. The two-dimensional (2D) object that identical to breast model is developed using numerical simulation to imitate the breast model. A filter is integrated with an iterative inversion technique for breast tumour detection to eliminate the noise. To assess the effectiveness of this approach, we consider the reconstruction of the electrical parameter profiles of 2D objects from measurements of the transient total electromagnetic field data contaminated with noise. Additive white Gaussian noise is utilized to mimic the effect of random processes that occur in the nature. This paper presents the filter settings and characteristics that affect the reconstruction of the image in order to obtain the most reliable and closer to the actual image. Selection of filter settings or design is important in order to achieve desired signal, most accurate image and provide reliable information of the object. Chebyshev low pass filter is applied in the Forward-Backward Time-Stepping (FBTS) algorithm to filter the noisy data and to improve the quality of reconstructed image.

Keywords: *Chebyshev low pass filter, microwave imaging and breast tumour detection*

----------***----------

1. INTRODUCTION

Breast cancer is the most cause of death among women. In 2014, an estimated 40,430 breast cancer deaths (40,000 women, 430 men), an estimated 232,670 new cases of invasive breast cancer were expected to be diagnosed, along with 62,570 new cases of non-invasive breast cancer (also known as carcinoma in situ) [1]. X-ray mammography [2], ultrasounds [3], combined [4] and in uncertain cases, with percutaneous (access the tissue by using needle-puncture) biopsy are the existing methods in detecting and screening breast cancer. As reported in [5], the limitations have inspire the researchers to develop another alternative detection method which is relatively safe, inexpensive imaging modality, and has ability to provide reliable and informative results. The main preventative strategy is focusing on the early detection and to improve the survival rates.

The last decade had shown significant increase involving microwave based system as reported in [6-10]. Microwave imaging is a technology which has potential application in diagnostic medical field. Microwave screening for breast cancer detection methods have been found to be more comfortable to the patient, low cost of scanning system and safe [11]. The ability to provide high contrast in dielectric properties of normal breast tissues and tumours have resulted in exploration of technique such as electrical microwave imaging via space-time (MIST) beamforming [12, 13], microwave tomography [10, 14] and radar based breast imaging [15-17].

At present, researchers are intriguing in designing and testing the efficiency of imaging system. The inversion method utilizing in time domain for reconstructing the electrical properties has been tremendously developed and improved [18-22]. The inverse scattering technique in electromagnetic has been investigated in various fields such as medical imaging [11], non-destructive evaluation [23-25], target identification [24-26] and geographical exploration [27].

Parallel computing [28] and random boundaries [29] have been applied to increase the efficiency of forward-backward time-stepping (FBTS) reconstruction method as the solution methods to overcome space limitation problem and to reduce the computation time.
In previous work in [30] had shown the capability of filtered FBTS applied for cancer breast detection with high contrast between fat and fibroglandular tissue, and low contrast between fibroglandular and tumour tissues. Noise degrades

the reconstructed image. In order to reduce the effect of noise, measured field data are filtered using low pass filter. In [8, 31], a new filtered FBTS algorithm has been developed to improve the quality of the image. Research works in [8, 30, 31] utilizing low pass filter in measured data have been done, which focusing on Chebyshev 4th order and frequency hopping technique to improve the quality of the reconstructed image.

In this research work, more aspects on Chebyshev filter in terms of characteristics, abilities and stability with the present of noise is observed. A number of numerical simulations with filtered FBTS algorithm at different order of Chebyshev at certain range of cut-off frequencies to be assessed in order to find reconstructed image closer to the actual image with minimum loss of higher frequency component of noise free data. The quality of image to be improved by utilizing filtered FBTS algorithm with parallel computing method to reduce computational time. The two-dimensional object that identical to breast model is developed using numerical simulation to imitate the breast model in which dielectric properties of the breast tissue is adopted.

2. METHODS

2.1 FBTS Algorithm

We consider inverse scattering problem where the electrical property distributions within a target object are estimated from scattering time domain data. This approach has potential to reconstruct the dielectric parameters more accurately and contains more quantitative information compared to single-frequency data. The finite-difference time-domain (FDTD) is conveniently utilized to reconstruct the two-dimensional image. The object is surrounded by sixteen antennas as illustrated in Figure 1. Each antenna takes turn to transmit a microwave pulse while the rest of antennas collect scattered signals until a set of transmitter/receiver data for multiple antenna combination is obtained. Then, this measured dataset is compared to an equivalent simulation in which the same set of scattering data is computed for an assumed set of dielectric parameters ***s*** representing the electrical properties profile of the breast tissue.

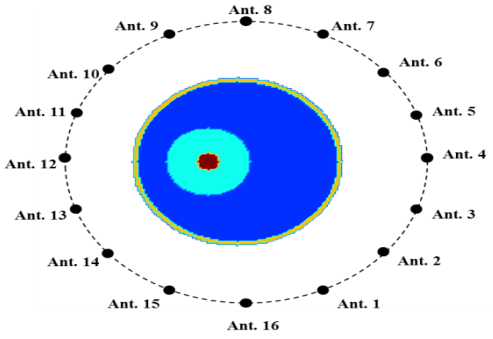

Fig -1: Configuration of the problem in 2-D

Figure 1 shows a two-dimensional dielectric breast model embedded in free space, illuminated by *M* short pulse waves generated by line current sources located at $\mathbf{r}_m^t$ (m = 1, 2,…, *M*). The problem considered here is to reconstruct the permittivity profile of the breast model from the knowledge of transient field data measured at several points $\mathbf{r}_n^t$ (n = 1, 2,…, *N*) for each illumination. The currents are assumed to point in the *z*-direction.

$$J_{zm}(\mathbf{r},t) = I(t)\delta(\mathbf{r} - \mathbf{r}_m^t) \tag{1}$$

where $\mathbf{r} = (x, y)$, $I(t)$ is a time factor, $\delta(\mathbf{r})$ is the Dirac delta function. We assume that the transmitter is turn on at time $t = 0$ and there is no electric fields before time $t = 0$.

The time factor, $I(t)$ is given by

$$I(t) = t_0 \left[\frac{d}{dt} \left(\frac{t}{t_0} \right)^4 e^{-\frac{t}{t_0}} \right] \tag{2}$$

Then, the total electromagnetic fields for the m^{th} current source satisfy the following Maxwell's equation in the matrix form which is given by

$$L\mathbf{b}_m = \mathbf{J}_m \tag{3}$$

with the initial condition

$$\mathbf{b}_m(\mathbf{r}, 0) = \mathbf{0} \tag{4}$$

Where

$$\mathbf{b}_m = \begin{pmatrix} E_{zm}(\mathbf{r},t) \\ \eta H_{xm}(\mathbf{r},t) \\ \eta H_{ym}(\mathbf{r},t) \end{pmatrix}, \qquad \mathbf{J}_m = \begin{pmatrix} J_{zm} \\ 0 \\ 0 \end{pmatrix} \tag{5}$$

The quantity $\eta = 1/\sqrt{\varepsilon_0 \mu_0}$ denotes the speed of light in free space and the operator L is given by

$$L \equiv \mathbf{A}\frac{\partial}{\partial x} + \mathbf{B}\frac{\partial}{\partial y} - \mathbf{C}\frac{\partial}{\partial t} \tag{6}$$

$$\mathbf{A} = \begin{pmatrix} 0 & 0 & 1 \\ 0 & 0 & 0 \\ 1 & 0 & 0 \end{pmatrix}, \mathbf{B} = \begin{pmatrix} 0 & -1 & 0 \\ -1 & 0 & 0 \\ 0 & 0 & 0 \end{pmatrix}, \quad \mathbf{C} = \begin{pmatrix} \boldsymbol{s} & 0 & 0 \\ 0 & 1 & 0 \\ 0 & 0 & 1 \end{pmatrix} \tag{7}$$

where **A** and **B** are constant matrices, **C** is matric consisting of the tensor of permittivity.

In this approach, the computed scattered signal dataset is calculated in time domain by utilizing FDTD technique to reconstruct the image. The cost functional $Q(\boldsymbol{s})$ for the assumed set of dielectric parameters $\boldsymbol{s}$ is expressed as

$$Q(\boldsymbol{s}) = \int_0^T \sum_{m=1}^{M} \sum_{n=1}^{N} W_{mn}(t) \left| \mathbf{b}_m(\boldsymbol{s}; \mathbf{r}_n, t) - \tilde{\mathbf{b}}_m(\mathbf{r}_n, t) \right|^2 dt \qquad (8)$$

where $\tilde{\mathbf{b}}_m(\mathbf{r}_n, t)$ and $\mathbf{b}_m(\boldsymbol{s}; \mathbf{r}_n, t)$ are the measured electromagnetic fields in the time domain at the receiver point $\mathbf{r}_n$ due to transmitter m and the corresponding calculated electromagnetic fields for an assumed set of dielectric parameters $\boldsymbol{s}$, respectively. The set of parameters $\boldsymbol{s}$ consists of the relative permittivity ε_r and the conductivity σ. $W_{mn}(t)$ is a non-negative weighting function which takes a value of zero at time $t = T$, where T is a time duration of the measurement.

When a gradient-based optimization method is applied to minimization of the cost functional in Eq. (8), the gradient of the functional is necessary. By taking the Fréchet derivative of Eq. (8), the gradients with respect to ε_r and σ are derived as

$$g_{\varepsilon_r}(\mathbf{r}) = \int_0^T \sum_{m=1}^{M} \boldsymbol{u}_m(\boldsymbol{s}; \mathbf{r}, t) \frac{d}{dt} \mathbf{b}_m(\boldsymbol{s}; \mathbf{r}, t)\, dt \qquad (9)$$

$$g_{\sigma}(\mathbf{r}) = \int_0^T \sum_{m=1}^{M} \boldsymbol{u}_m(\boldsymbol{s}; \mathbf{r}, t) \mathbf{b}_m(\boldsymbol{s}; \mathbf{r}, t)\, dt \qquad (10)$$

where the electromagnetic fields $\mathbf{b}_m(\boldsymbol{s}; \mathbf{r}, t)$ and the adjoint fields $\boldsymbol{u}_m(\boldsymbol{s}; \mathbf{r}, t)$ calculated in the reconstruction region. The adjoint fields $\boldsymbol{u}_m(\boldsymbol{s}; \mathbf{r}, t)$ are time reversed fields with equivalent current sources which are identical to a difference between the measured and calculated scattered field data. In this paper, we used Polak-Ribière-Polyak conjugate gradient method for optimization technique to solve the inverse scattering problem.

2.2 Filtered FBTS Algorithm

In practice, measured data is usually contaminated with noise and each time of assessment the noise could be different. Additive white Gaussian noise is added in the measured field data. The noise normally has higher frequency spectrum compared to spectrum of the field data due to decorrelatedness of noise. The signal-to-noise ratio (SNR) is defined as follows:

$$\mathrm{SNR} = 10 \log_{10} \frac{\sum_{m=1}^{M} \sum_{n=1}^{N} \int_0^T \left| \tilde{\mathbf{b}}_{m'}(\mathbf{r}_n^t, t) \right|^2 dt}{\sum_{m=1}^{M} \sum_{n=1}^{N} \int_0^T \left| \Omega_{m'}(\mathbf{r}_n^t, t) \right|^2 dt} \qquad (11)$$

where $\Omega_{m'}(\mathbf{r}_n^t, t)$ is noise added to the measured electromagnetic fields at $\tilde{\mathbf{b}}_{m'}(\mathbf{r}_n^t, t)$.

To eliminate the noise effects, noisy data is filtered with a Chebyshev low pass filter which the amplitude response is expressed by

$$H(f) = \frac{1}{\sqrt{1 + \epsilon^2 [T_k(f)]^2}} \qquad (12)$$

where ϵ is the ripple factor, $f = \frac{f_0}{f_{c0}}$, f_{co} is cut-off frequency, f_c is the center frequency. $T_k(f)$ is the k^{th} order Chebyshev polynomial which is given by

$$T_k(f) = \begin{cases} \cos\left[k \cos^{-1}\left(\frac{f_0}{f_{c0}} \right) \right] & \left| \frac{f_0}{f_{c0}} \le 1 \right| \\ \cosh\left[k \cosh^{-1}\left(\frac{f_0}{f_{c0}} \right) \right] & \left| \frac{f_0}{f_{c0}} > 1 \right| \end{cases} \qquad (13)$$

The general expression for the transfer function of k^{th} order of Chebyshev low pass filter is given by

$$H(x) = \frac{H_0}{\prod_{i=1}^{k} (x - x_i)} = \frac{H_0}{\prod_{i=1}^{k} (x - x_1)(x - x_2) \ldots (x - x_k)} \qquad (14)$$

Where

$$H_0 = \begin{cases} \prod_{i=1}^{k} (-x_i) & k \text{ odd} \\ 10^{\frac{r}{20}} \prod_{i=1}^{k} (-x_i) & k \text{ even} \end{cases} \qquad (15)$$

To compute the pole values (x_1, x_2, x_3, ...) of k^{th} order Chebyshev low pass filter

$$x_i = \alpha_i + j\beta_i \qquad (16)$$

$$\alpha_i = \left[\frac{\left(\frac{1}{\gamma} - \gamma \right)}{2} \right] \sin \frac{(2i-1)\pi}{2k} \qquad (17)$$

$$\beta_i = \left[\frac{\left(\frac{1}{\gamma} + \gamma \right)}{2} \right] \cos \frac{(2i-1)\pi}{2k} \qquad (18)$$

$$\gamma = \left(\frac{1+\sqrt{1+\epsilon^2}}{\epsilon} \right)^{\frac{1}{k}} \quad (19)$$

To determine the ripple factor ϵ, Eq. (20) is used.

$$\epsilon^2 = 10^{\frac{r}{10}} - 1 \quad (20)$$

where r is the ripple size in dB.

Table - 1: Chebyshev Polynomials

k^{th} order of Chebyshev	Factors of the Denominator
1	$(x + 1.00238)$
2	$(x^2 + 0.64490x + 0.70795)$
3	$(x + 0.29862)(x^2 + 0.29862x + 0.83917)$
4	$(x^2 + 0.17034x + 0.90309)(x^2 + 0.41124x + 0.19598)$
5	$(x + 0.17753)(x^2 + 0.10970x + 0.93603)(x^2 + 0.28725x + 0.37701)$

Table 1 shows the factors of the denominator polynomials normalized Chebyshev low pass filter. In order to assess the functionality of the filter, the calculated fields also to be passed through the same procedure which has the same low pass filter characteristic. High frequency noise effects can be reduced by filtering with low pass filter. The measured field data are first low pass filtered and the FBTS algorithm is applied to the filtered data. Then, the filtered version of cost functional in Eq. (8) yields:

$$Q(s) = \int_0^T \sum_{m=1}^{M} \sum_{n=1}^{N} W_{mn}(t) \left| \mathbf{B}_m(\mathbf{s}; \mathbf{r}_n^r, t) - \tilde{\mathbf{B}}_m(\mathbf{r}_n^r, t) \right|^2 dt \quad (21)$$

2.3 Parallel Computing

The FBTS algorithm is implemented in C++ language executed in parallel computing. Parallel computing can be divided into two types, shared memory and distributed memory. Shared memory is performed by a computer with a number of processor and shared the memory while distributed memory is performed by a number of computers which each computer has its own processor with own memory. The transmission and reception of the data between the computers are made via interconnection network. In this simulation works, distributed memory parallel computing is used by utilizing a cluster of 8 computers to minimize the calculation time.

The cost functional, Q_P for parallel filtered FBTS is expressed by

$$\boldsymbol{Q}_P(\boldsymbol{s}) = \sum_{c=1}^{C} \int_0^T \sum_{m=1}^{M'} \sum_{n=1}^{N} W_{m'n}(t) \left| \mathbf{B}_{m'}(\boldsymbol{s}; \mathbf{r}_n^r, t) - \tilde{\mathbf{B}}_{m'}(\boldsymbol{s}; \mathbf{r}_n^r, t) \right|^2 dt \quad (22)$$

where C is the number of computers, M' is the number of transmitter points assigned to a computer. Therefore, the number of M in Eq. (8) is related to the number of M' and C in Eq. (22). M is the total number of transmitter points which is expressed $M = C \times M'$.

The gradient vector, G_P (r) can be rewritten as

$$G_{P_{\varepsilon_r}} = \sum_{c=1}^{C} \left\{ 2 \int_0^T \sum_{m'=1}^{M'} \sum_{n=1}^{3} u_{m'}(\boldsymbol{s}; \mathbf{r}, t) \frac{\partial}{\partial(t)} \boldsymbol{b}_{m'}(\boldsymbol{s}; \mathbf{r}_n^r, t) d(t) \right\} \quad (23)$$

$$\mathrm{G}_{P_\sigma} = \sum_{c=1}^{C} \left\{ 2 \int_0^T \sum_{m'=1}^{M'} \sum_{n=1}^{3} u_{m'}(\boldsymbol{s}; \mathbf{r}, t) \boldsymbol{b}_{m'}(\boldsymbol{s}; \mathbf{r}_n^r, t) d(t) \right\} \quad (24)$$

3. RESULTS AND DISCUSSION

In this research work, we used a Chebyshev low pass filter of k = 2, 3, 4 and 5, with cut-off frequency of 1.5GHz and ripple size of 3dB. The model was resized to a resolution of 1mm × 1mm. Fixed skin layer of 2mm thickness was added in the model. The grid size for the FDTD was 1mm × 1mm. The excitation signal sinusoidally modulated Gaussian pulse with a center frequency, f_c = 2GHz and bandwidth of 1.3GHz are used in the FBTS reconstruction algorithm. The optimization was carried out up to 30 iterations utilizing 16 antennas to reconstruct the image.

The size of the tumour embedded in the fibroglandular tissue of breast model is 10mm in diameter. The initial guess for ε_r and σ values in the entire reconstruction region (including fat, fibroglandular and skin tissues) are 13.7 and 0.10, respectively. Nominal Debye parameters for the breast tissues used in this paper are summarized in Table 2.

Table -2: Electrical properties of breast tissues

Tissue	ε_s	ε_∞	σ_s	τ	ε_r (2GHz)	σ (2GHz)
Fibrograndular	21.57	6.14	0.31	7.0e-12	21.45	0.46
Fat	10.00	7.00	0.15	7.0e-12	9.98	0.18
Skin	37.00	4.00	1.10	7.2e-12	36.73	1.40
Tumour	54.00	4.00	0.70	7.0e-12	53.62	1.19

The foundation of this approach is formulated utilizing Debye equation. The Debye equation can be expressed as

$$\varepsilon^*(\omega) = \varepsilon_\infty + \frac{\varepsilon_s - \varepsilon_\infty}{1 + j\omega\tau} - j\frac{\sigma_s}{\omega\varepsilon_0} \quad (25)$$

where ε_∞ is the relative permittivity at infinite frequency, ε_s is the static relative permittivity, τ is the relaxation time, and σ_s is the static conductivity.

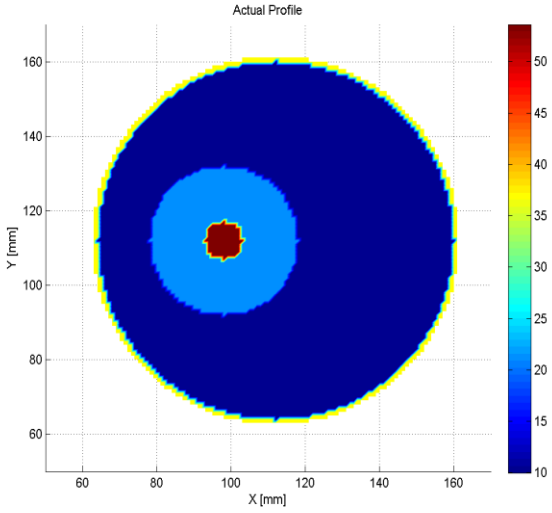

(a)

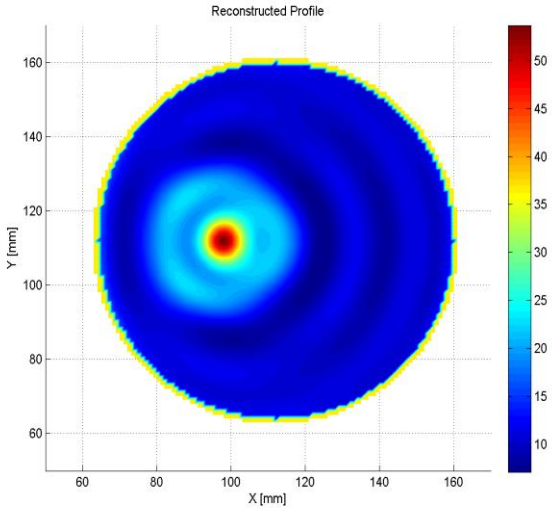

(b)

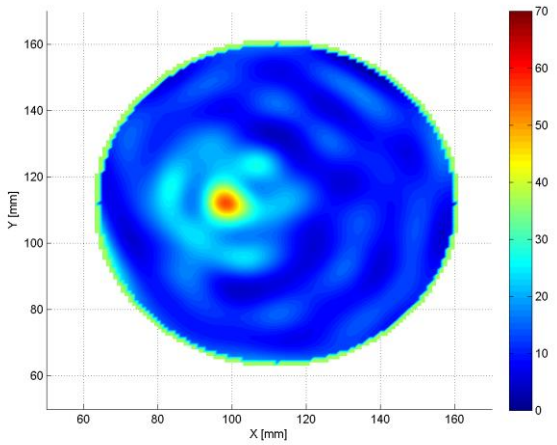

(c)

Fig -2: Permittivity images in *xy* plane (*x*=98mm) of breast model with 10mm size of tumour embedded in the fibroglandular region. (a) Actual image. (b) Reconstructed image from noise-free data. (c) Reconstructed image from noisy-data with SNR -3dB.

Figure 2(a) illustrates the actual image of numerical breast model while Figure 2(b) presents the reconstructed relative permittivity image with noisy-free data. The reconstructed image after 10 iterations is very close to the original profile. The reconstructed image from the contaminated data has been poor where the fibroglandular region has been distorted as shown Figure 2(c). The background medium free space is used as an initial guess in the reconstruction.

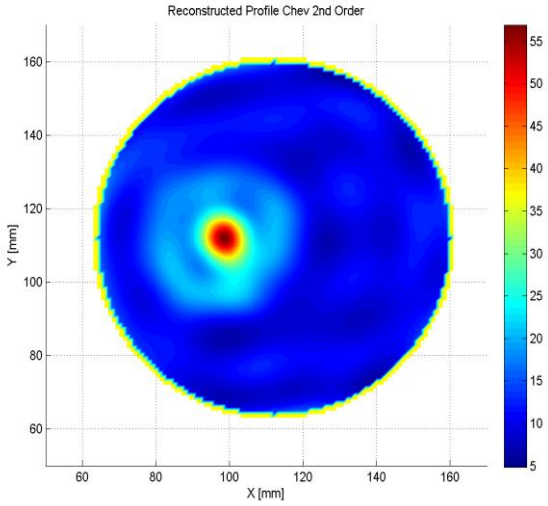

(a)

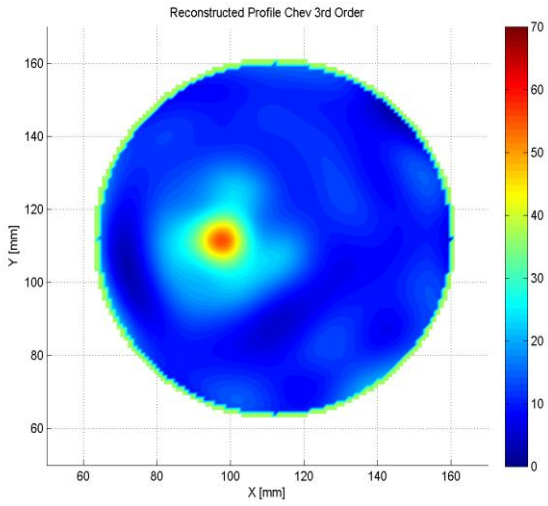

(b)

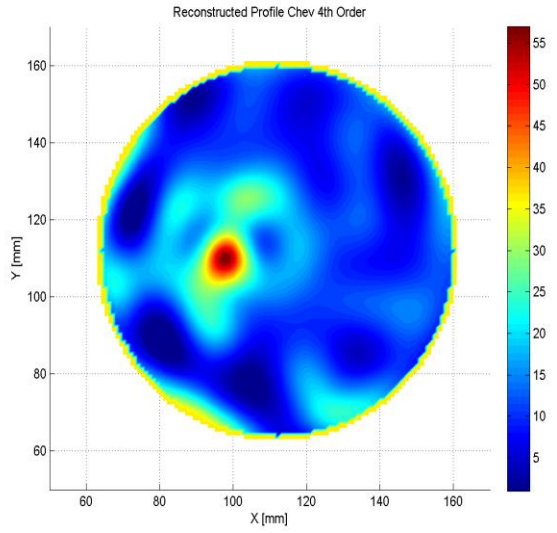

(c)

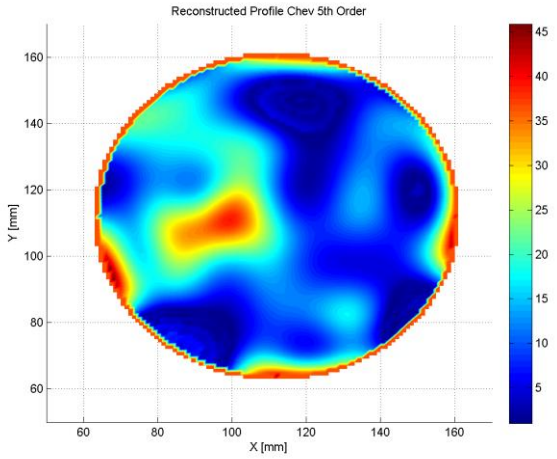

(d)

Fig -3: Permittivity images of breast like model with 10mm size of tumour embedded in the fibroglandular region: (a) Chebyshev 2nd Order, (b) Chebyshev 3rd Order, (c) Chebyshev 4th Order, and (d) Chebyshev 5th Order.

Figure 3 shows reconstructed image from noisy data after 10th iteration using Chebyshev filter, k = 2, 3, 4 and 5, respectively. The tumour is clearly detected and distinct from the surrounding breast tissue as shown Figure 3(a) through Figure 3(c). Reconstructed profile approximately accurate using 2nd order of Chebyshev filter as shown in Figure 3(a). However, the fibroglandular region is saturated using 5th order of Chebyshev filter due to large amount of spectral component of the measured data are lost by the filter as shown in Figure 3(d).

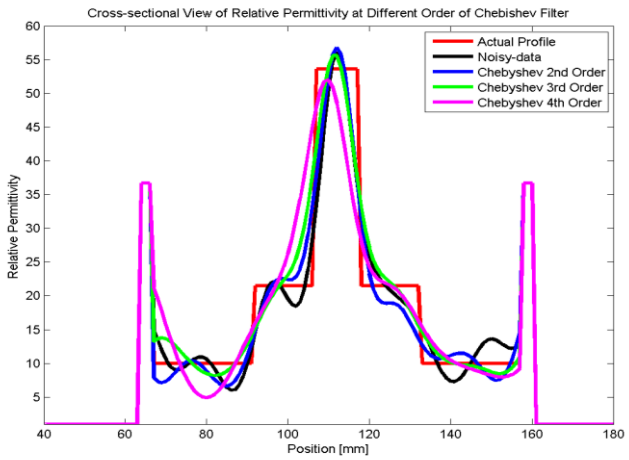

Fig -4: Cross sectional view along the x-axis (x=96mm) simulated image with 10mm size of tumour embedded in the numerical breast model.

Figure 4 shows the cross-sectional view along the vertical line (x=96mm) through the center of the tumour. For simple homogeneous model, Chebyshev 2nd order filter has shown the closes to the actual value while higher order has shown the reconstructed image has been saturated due loss of high spectrum of noise-free data.

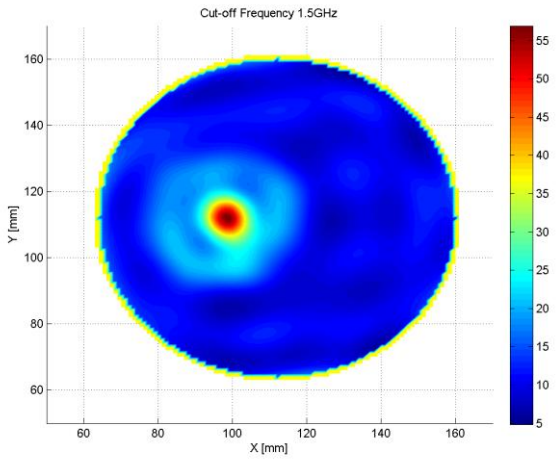

(a)

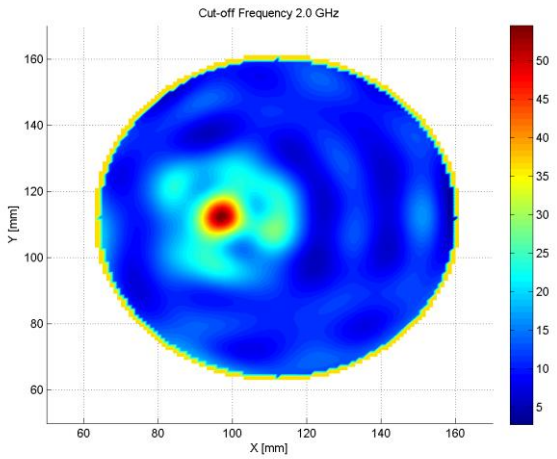

(b)

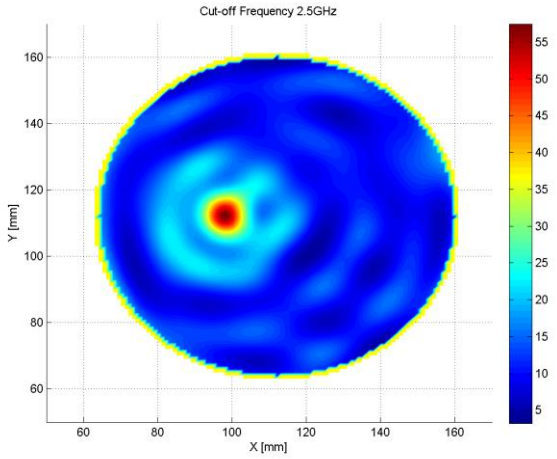

(c)

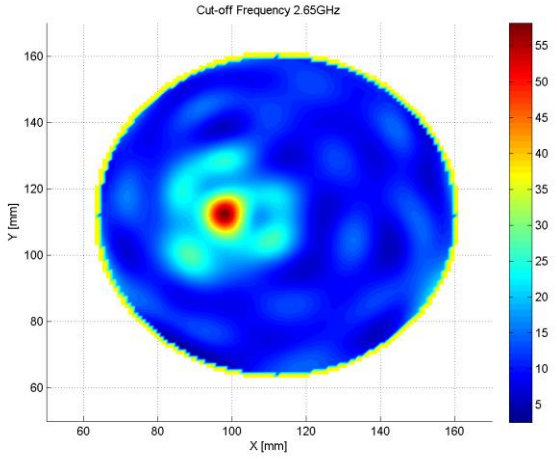

(d)

Fig -5: Reconstruction of permittivity images of breast model with 5mm size of tumour embedded in the fibroglandular region using filtered FBTS with 2nd Order of Chebyshev low pass filter at different cut-off frequency: (a) 1.5GHz, (b) 2.0GHz, (c) 2.5GHz, and (d) 2.65GHz

Chebyshev 2nd order is selected as the reconstructed image shows more nearer to the actual value compared to 3rd, 4th and 5th order. In order to find reconstructed image closer to the actual image with minimum loss of higher frequency component of noise-free data, further investigation has been made at selected cut-off frequencies as demonstrated in Figure 5. The highest cut-off frequency allows the maximum range of reception at the receiver point.

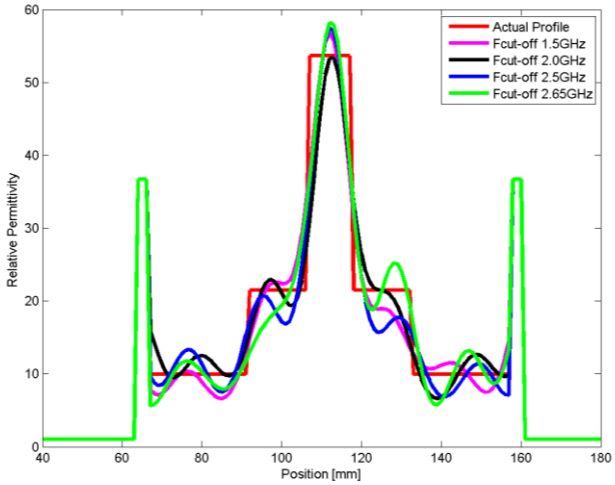

Fig -6: Cross sectional view along the *x*-axis (*x*=98mm) simulated image at different cut-off frequency.

High frequency effects have been reduced by using 2nd order of Chebyshev low pass filter with cut-off frequency 2.65GHz. In this research work, a sinusoidal modulated pulse with center frequency 2GHz and bandwidth of 1.3GHz has been used. Maximum measured field data can be retrieved at the maximum bandwidth using the highest cut off-frequency which allows the maximum reception at the receiver point.

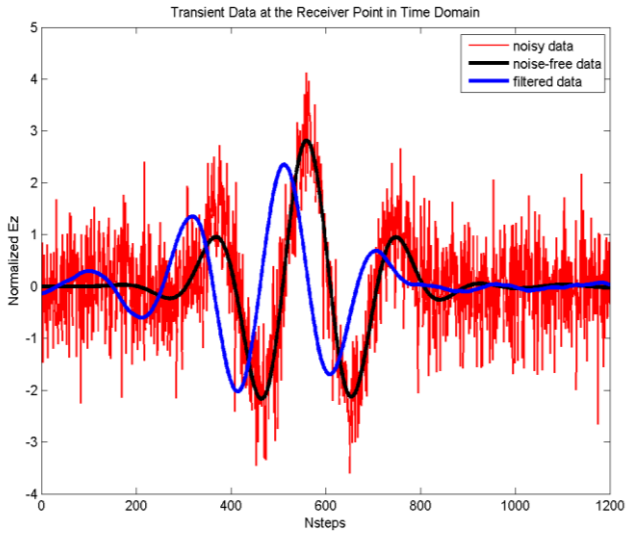

Fig -7: Transient filed data at the receiver point for homogeneous breast model. The thick solid curve denotes noise-free data while the thin solid curve represents noise-contaminated field data with SNR -3dB.

4. CONCLUSION AND FUTURE WORKS

The results from this research have shown that the low pass filter applied in FBTS has been successfully in eliminating the noise and detecting the tumour. Noise has higher spectrum than the spectrum of the field data. High frequency effects can be reduced by using low pass filter at range of 1.5GHz to 2.65GHz for homogeneous model. Although the Chebyshev low pass filter has been successful in eliminating

the noise, there were large amount of spectral components of the measured data are lost by using filter. In this simple homogeneous breast model, the lower order of Chebyshev polynomial is sufficient enough to filter out the noise. Next we consider using the band pass filter or combination both of low pass filter and band pass filter to minimize the loss of higher frequency components of noise-free field data. The filter settings are adjustable at various order of low pass filter at selected cut-off frequency in order to obtain the most reliable and informative results which nearer to the original profile. Obtaining this relation, we also consider to investigate the stability and capability of filtered FBTS in various medium such as corn syrup, saline and sodium meta silicate (SMS) gel.

ACKNOWLEDGEMENTS

The authors would like to thank to Faculty of Engineering for assistant in providing facilities used for this project. This research work was supported by OSAKA GAS FOUNDATION IN CULTURAL EXCHANGE (OGFICE) Research Grant Scheme. The authors also thank reviewers for their valuable comments and suggestions.

REFERENCES

[1] "*Cancer Fact and Figure"*. Available: http://www.cancer.org/acs/groups/content/@research/documents/webcontent/acspc-042151.pdf, [Accessed: 2015 March 14].

[2] L. Lihua, W. Zuobao, C. Li, F. George, C. Zhao, A. Salem, M. Kallergi, and C. Berman, "Breast tissue density and CAD cancer detection in digital mammography," presented at the Engineering in Medicine and Biology Society, 2005. IEEE-EMBS 2005. 27th Annual International Conference of the IEEE Engineering in Medicine and Biology Society, 2005.

[3] M. C. Purdy."*Ultrasound Screening Finds More Breast Cancer, False Positives May Outweigh That Benefit"*. [Online]. Available: http://news.wustl.edu/news/Pages/23668.aspx, [Accessed: 2014 April 4].

[4] W. A. Berg, J. D. Blume, J. B. Cormack, E. B. Mendelson, D. Lehrer, M. Böhm-Vélez, E. D. Pisano, R. A. Jong, W. P. Evans, and M. J. Morton, "Combined screening with ultrasound and mammography vs mammography alone in women at elevated risk of breast cancer," *Jama*, vol. 299, pp. 2151-2163, 2008.

[5] S. V. Sree, E. Y.-K. Ng, R. Acharya U, and W. Tan, "Breast imaging systems: A review and comparative study," *Journal of Mechanics in Medicine and Biology*, vol. 10, pp. 5-34, 2010.

[6] X. Li and S. C. Hagness, "A confocal microwave imaging algorithm for breast cancer detection," *Microwave and Wireless Components Letters, IEEE*, vol. 11, pp. 130-132, 2001.

[7] V. Zhurbenko, T. Rubæk, V. Krozer, and P. Meincke, "Design and realisation of a microwave three-dimensional imaging system with application to breast-cancer detection," *IET Microwaves, Antennas & Propagation*, vol. 4, p. 2200, 2010.

[8] T. Tanaka, N. Kuroki, and T. Takenaka, "Filtered forward-backward time-stepping method applied to reconstruction of dielectric cylinders," *Journal of Electromagnetic Waves and Applications*, vol. 17, pp. 253-270, 2003/01/01 2003.

[9] M. Lazebnik, D. Popovic, L. McCartney, C. B. Watkins, M. J. Lindstrom, J. Harter, S. Sewall, T. Ogilvie, A. Magliocco, T. M. Breslin, W. Temple, D. Mew, J. H. Booske, M. Okoniewski, and S. C. Hagness, "A large-scale study of the ultrawideband microwave dielectric properties of normal, benign and malignant breast tissues obtained from cancer surgeries," *Physics in Medicine and Biology*, vol. 52, pp. 6093-115, Oct 21 2007.

[10] S. Semenov, "Microwave tomography: review of the progress towards clinical applications," *Philosophical Transactions of the Royal Society A: Mathematical, Physical and Engineering Sciences*, vol. 367, pp. 3021-42, Aug 13 2009.

[11] J. E. Johnson, T. Takenaka, K. Hong Ping, S. Honda, and T. Tanaka, "Advances in the 3-D forward-backward time-stepping (FBTS) inverse scattering technique for breast cancer detection," *Biomedical Engineering, IEEE Transactions on*, vol. 56, pp. 2232-2243, 2009.

[12] X. Li, S. K. Davis, S. C. Hagness, D. W. Van Der Weide, and B. D. Van Veen, "Microwave Imaging via Space Time Beamforming : Experimental Investigation of Tumor Detection in Multilayer Breast Phantoms," *Microwave Theory and Techniques, IEEE Transactions on Bio-medical Engineering*, vol. 52, pp. 1856-1865, 2004.

[13] E. J. Bond, X. Li, S. C. Hagness, and B. D. Van Veen, "Microwave Imaging via Space-Time Beamforming for Early Breast Cancer Detection," *Antennas and Propagation, IEEE Transactions on Bio-medical Engineering*, vol. 51, pp. 1690-1705, 2003.

[14] A. H. Barrett, P. C. Myers, and N. L. Sadowsky, "Microwave thermography in the detection of breast cancer," *AJR Am J Roentgenol*, vol. 134, pp. 365-8, Feb 1980.

[15] S. J. A. G. N. Bindu, A. Lonappan, V. Thomas, C. K. Aanandan, and K. T. Mathew, "Active microwave imaging for breast cancer detection," *Progress In Electromagnetics Research* vol. 58, pp. 149–169, 2006.

[16] S. C. Hagness, A. Taflove, and J. E. Bridges, "Two-dimensional FDTD analysis of a pulsed microwave confocal system for breast cancer detection: Fixed-focus and antenna-array sensors," *IEEE Transactions on Biomedical Engineering*, vol. 45, pp. 1470-1479, 1998.

[17] E. C. Fear and M. A. Stuchly, "Microwave detection of breast cancer," *IEEE Transactions on Microwave Theory and Techniques*, vol. 48, pp. 1854-1863, 2000.

[18] P. Kosmas, "Application of the DORT technique to FDTD-based time reversal for microwave breast cancer detection," in *Microwave Conference, 2007. European*, 2007, pp. 306-308.
[19] S. Caorsi and G. L. Gragnani, "Inverse-scattering method for dielectric objects based on the reconstruction of the nonmeasurable equivalent current density," *Radio Science*, vol. 34, pp. 1-8, 1999.
[20] T. Takenaka, H. Jia, and T. Tanaka, "Microwave imaging of electrical property distributions by a forward-backward time-stepping method," *Journal of Electromagnetic Waves and Applications*, vol. 14, pp. 1609-1626, 2000.
[21] J. Hongting and K. Yasumoto, "Time domain inverse scattering analysis of stratified lossy media using a forward-backward time-stepping method," in *2004 3rd International Conference on Computational Electromagnetics and Its Applications, Proceedings. ICCEA 2004.* , 2004, pp. 415-418.
[22] H. Zhou, T. Takenaka, J. E. Johnson, and T. Tanaka, "A breast imaging model using microwaves and a time domain three dimensional reconstruction method," *Progress In Electromagnetics Research*, vol. 93, pp. 57-70, 2009.
[23] S. Caorsi, A. Massa, M. Pastorino, and M. Donelli, "Improved microwave imaging procedure for nondestructive evaluations of two-dimensional structures," *IEEE Transactions on Antennas and Propagation*, vol. 52, pp. 1386-1397, 2004.
[24] Y. Altuncu, F. Akleman, O. Semerci, and C. Ozlem, "Imaging of dielectric objects buried under a rough surface via distorted born iterative method," *Journal of Physics: Conference Series*, vol. 135, p. 012006, 2008.
[25] M. Pastorino, A. Salvade, R. Monleone, T. Bartesaghi, G. Bozza, and A. Randazzo, "Detection of defects in wood slabs by using a microwave imaging technique," in *Instrumentation and Measurement Technology Conference Proceedings, 2007. IMTC 2007. IEEE*, 2007, pp. 1-6.
[26] C. Wei, H. Chung-Hsin, L. Chun Jen, and C. Chien-Ching, "Inverse problem of a buried metallic object," in *Microwave Conference, European*, 2005, p. 4 pp.
[27] T. J. Cui, C. Weng Cho, A. A. Aydiner, and C. Siyuan, "Inverse scattering of two-dimensional dielectric objects buried in a lossy earth using the distorted Born iterative method," *IEEE Transactions on Geoscience and Remote Sensing*, vol. 39, pp. 339-346, 2001.
[28] T. Moriyama, Y. Yamaguchi, K. Hong Ping, T. Tanaka, and T. Takenaka, "Parallel processing of forward-backward time-stepping method," *Progress In Electromagnetics Research*, vol. 4, pp. 695-700, 2008.
[29] H. Zhou and H. Zhang, "Increasing the efficiency of forward–backward time-stepping reconstruction method," in *Proceedings of Progress In Electromagnetics Research Symposium, China, Suzhou*, 2011, pp. 878-881.
[30] T. Takenaka, T. Moriyama, K. Hong Ping, and T. Yamasaki, "Microwave breast imaging by the filtered forward-backward time-stepping method," in *URSI International Symposium on Electromagnetic Theory (EMTS)*, 2010, pp. 946-949.
[31] K. Hayashi, T. Tanaka, T. Takenaka, and H. Zhou, "Filtered forward-backward time-stepping method applied to borehole radar imaging," in *Proc. URSI Int. Symp. on Electromagnetic Theory*, 2004, pp. 804-806.

BIOGRAPHIES

Marta a/p Elizabeth currently PG student, Department of Electrical and Electronic Engineering. She received her B. Eng (Hons) degree in Electronics and Telecommunication Engineering from Universiti Malaysia Sarawak, Malaysia.

Kismet Anak Hong Ping received his PhD in System Science from Nagasaki University, Japan. MSc in Digital Communication System from Loughborough University, UK and B. E (Hons) in Electronics and Telecommunication Engineering, Universiti Malaysia Sarawak, Malaysia.

Nordiana binti Rajaee received her PhD in DNA Computing from Meiji University, Japan. MSc in Microelectronic from University of Newcastle Upon Tyne and B. Eng (Hons) in Electronic and Information Engineering from Kyushu Institute of Technology, UK.

Toshifumi Moriyama received his B.E., M.E., and D.E. degrees in Information Engineering all from Niigata University, Japan. He currently an Associate Professor at Nagasaki University, Nagasaki, Japan